Supplemental Materials:

Materials and Methods

Model of CHE

An established rat model of experimental CHE was used in this study (Schmandra *et al*. 2001; Singh and Trigun 2010). Briefly, CHE was induced in adult rats (Fisher-344, 160-175 gm) following the intraperitoneal injection of the liver toxin thioacetamide (100 mg TAA/kg b. wt. prepared in 0.9% NaCl) for 10 consecutive days. Control rats were given the same volume of 0.9% NaCl. To minimize weight loss, hypoglycemia, dehydration and renal failure in TAA-treated rats, 5% dextrose containing 0.45% NaCl and 20 mEq/L of potassium chloride were added to the drinking water.

Previous reports of this model have described hepatic damage (increased blood levels of alanine aminotransferase and aspartate aminotransferase, as well as histopathological changes in the liver); alterations in brain biochemical parameters (increase in neuronal nitric oxide synthase, NADPH oxidase activity, over-activation of glucose-6-phosphate dehydrogenase, and a decline in phosphofructokinase-2); as well as behavioral abnormalities characteristic of CHE (Schmandra *et al*. 2001; Singh and Trigun 2010).

To further characterize this model of CHE, liver and brain morphological changes, as well as blood and brain ammonia levels were examined as described previously (Rama Rao *et al*. 2010). Blood and brain cortical ammonia concentration were significantly increased in TAA-treated rats (two- to three-fold) (see Table). Ammonia levels in blood and brain tissue of these rats were comparable with those found in rats after portocaval anastomosis (Butterworth *et al*. 1988; Dejong *et al*. 1993). Liver and brain from control and TAA-treated rats were fixed in 10% formalin for 24 h, processed routinely for paraffin sections and stained with hematoxylin and eosin (H&E). Liver sections from TAA-treated rats showed ballooning degeneration, hydropic changes and the presence of eosinophilic bodies, affecting approximately 60-70% of the liver parenchyma, predominantly in periportal regions (figures not shown). We also identified the presence of Alzheimer type II astrocytosis in the cerebral cortex (Suppl. Figure 1). Additionally, behavioral abnormalities associated with cognitive dysfunction that are

similar to those in humans with CHE were observed, including drowsiness, decreased wakefulness, attentiveness, grooming and exploratory behavior. While the CHE animals are behaviorally defective, no evidence of severe distress, such as intense pain, muscular spasms, fainting or breathing difficulties were noticed. These findings demonstrate that a low dose of TAA administered for 10 days reproduces many of the features associated with CHE in humans, consistent with observations by other investigators (Schmandra *et al*. 2001; Singh and Trigun 2010).

Transfection of cultures with siRNAs

Rat c-Myc specific siRNA (cat#sc-270149, Santa Cruz Biotechnology, Dallas, TX), was used in this study, while scrambled siRNA (cat#sc-37007, Santa Cruz Biotechnology) was used as control. Transfection of siRNAs in astrocyte cultures was carried out using the 'TransIT-TKO' transfection reagent (cat#MIR 2150; Mirus, Madison, WI, USA) as described previously (Jayakumar *et al*. 2011). The TransIT-TKO transfection reagent was diluted without serum and incubated at 37°C for 30 min, followed by the addition of siRNA, and incubation at 37°C for another 30 min. The siRNA/TransIT-TKO complex was diluted in medium containing 10% horse serum, and then added to the astrocyte cultures. Transfection times and siRNA concentrations for optimal transfection was tested using different concentrations of siRNA (10-200 nM), and different transfection incubation times (24–96 h) (Jayakumar *et al.* 2011). c-Myc silencing was confirmed by real-time quantitative PCR (RT-qPCR) and Western blots.

RNA isolation and RT-qPCR

RNA was isolated using RNAqueous®-4PCR kit (#AM1914; Ambion, Austin, TX) as described previously (Jayakumar et al., 2011). Briefly, 2 μg RNA was used to generate cDNA with a High Capacity cDNA Reverse Transcription Kit (catalog #4368814; Applied Biosystems, Foster City, CA). RT-qPCR was carried out using 10 μL diluted cDNA (1:20 dilution) on the Mx3005P Multiplex Quantitative PCR System (catalog #401513; Stratagene/Agilent Technologies, Wilmington, DE) with RT-qPCR SYBR GREEN Reagents (Brilliant® II SYBR® Green QPCR Master Mix; Agilent Technologies) and ROX as a reference dye (final reaction volume 25 μL). RT-qPCR cycling conditions were: (1) 95°C for 10 min, (2) 40 cycles of 95°C for 30 s, 58°C for 30 s, and (3) 72°C for 15 s. The MxPro-

Mx3005P v4.10 software (Stratagene/Agilent Technologies, Wilmington, DE) was used to determine the crossing points for each amplification reaction. TSP-1 mRNA primer pairs (NM_001013062.1); Forward: 5′-GGAGGTGCCCGCAAGGTTCC-3′, Reverse: 5′-TTGTCGGCCCACACAGCGTC-3′). All RT-qPCR data were normalized against the ribosomal protein large subunit 13a mRNA (RPL13a, NM_173340; Forward: 5′-GGCTGAAGCCTACCAGAAAG-3′; Reverse: 5′-CTTTGCCTTTTCCTTCCGTT-3′).

Immunoblotting

After treatment with ammonium chloride (ammonia, 0.5-2.5 mM), culture media were collected, and cells lysed with 125 mM Tris-HCl 6.8; 4% SDS, and a protease inhibitor mixture (Roche Products, Indianapolis, IN). The collected media were concentrated with an Amicon Ultra 4 centrifugal filter device having a 10,000 molecular weight cutoff (Millipore, Billerica, MA), according to the manufacturer's instructions. Protein concentrations were measured by the BCA method. Equal amounts of protein were subjected to SDS-PAGE using 4-20% gels (Tris-HCl) and then electrophoretically transferred to a PVDF membrane. Blots were blocked with 5% BSA in TBS-T (TBS; 20 mM Tris-HCl, 150 mM NaCl, pH 7.4, and 0.05% Tween 20) for 2 h at RT and then incubated with respective primary antibodies at 4°C overnight. Membranes were washed with TBS-T and incubated with HRP-conjugated secondary antibodies for 2 h at RT. After washing, membranes were visualized using enhanced chemiluminescence reagents (ECL-plus; Amersham Biosciences, Piscataway, NJ). Primary antibodies to detect TSP-1 (mouse monoclonal antibody A6.1, cat#BA24, Ab-3) and TGF-β1 (Ab-1, Mouse mAb, 9016.2) were purchased from Calbiochem (Millipore, Billerica, MA). Primary antibodies to detect SPARC-like 1 (hevin, Cat#13517-1-AP) was purchased from Proteintech Group, Inc. Chicago, IL; PSD95 (D27E11) XP® Rabbit mAb (cat#3450) was purchased from Cell Signaling Technology (Danvers, MA); synaptophysin antibody was obtained from Abcam (YE269, ab32127, Cambridge, MA); synaptotagmin 1(15) (cat#sc-136480) was purchased from Santa Cruz Biotechnology, Dallas, TX; and anti-α- and β-tubulin antibodies were obtained from Oncogene (San Diego, CA) and Sigma-Aldrich (St. Louis, MO). All primary antibodies were used at 1:1000 dilutions.

Anti-rabbit and anti-mouse (Vector Laboratories, Burlingame, CA) HRP-conjugated secondary antibodies were used at 1:1000. Optical density of the bands was measured with the

Chemi-Imager digital imaging system (Alpha Innotech, San Leandro, CA), and the results were quantified with Sigma Scan Pro (St. Louis, MO) as a proportion of the signal of a house-keeping protein band (α-tubulin, for astrocytes and β-tubulin for neurons). Controls, which included omission of the primary antibodies, did not show a band.

References:

Butterworth R. F., Girard G. and Giguère J. F. (1988) Regional differences in the capacity for ammonia removal by brain following portocaval anastomosis. *J. Neurochem.* 51, 486-490.

Dejong C. H., Deutz N. E. and Soeters P. B. (1993) Cerebral cortex ammonia and glutamine metabolism in two rat models of chronic liver insufficiency-induced hyperammonemia: influence of pair-feeding. *J. Neurochem.* 60, 1047-1057.

Jayakumar A. R., Panickar K. S., Curtis K. M., Tong X. Y., Moriyama M. and Norenberg M. D. (2011) Na-K-Cl cotransporter-1 in the mechanism of cell swelling in cultured astrocytes after fluid percussion injury. *J. Neurochem.* 117, 437-448.

Rama Rao K. V., Reddy P .V., Tong X. and Norenberg M. D. (2010) Brain edema in acute liver failure: inhibition by L-histidine. *Am. J. Pathol.* 176, 1400-1408.

Schmandra T. C., Bauer H., Petrowsky H., Herrmann G., Encke A. and Hanisch E. (2001) Effects of fibrin glue occlusion of the hepatobiliary tract on thioacetamide-induced liver failure. *Am. J. Surg.* 182, 58-63.

Singh S. and Trigun S. K (2010) Activation of neuronal nitric oxide synthase in cerebellum of chronic hepatic encephalopathy rats is associated with up-regulation of NADPH-producing pathway. *Cerebellum* 9, 384-397.

FIGURE LEGENDS

FIGURE 1. Histopathological changes in the cerebral cortex of rats treated with thioacetamide (TAA) for 10 days. (*A*) Photomicrograph of normal rat cerebral cortex showing normal astrocyte nuclei (arrows). (*B*) Photomicrograph of cerebral cortex from rats treated with TAA. Astrocytic nuclei are enlarged and pale (arrows), often are found in pairs (crossed arrows), and display margination of nuclear chromatin, features characteristic of Alzheimer type II astrocytes. Neurons are morphologically intact in TAA-treated rats (arrowheads). Scale bar = 20 μm.

FIGURE 2. Intracellular TSP-1 level after a 5-day treatment of cultured astrocytes with 0.5-2.5 mM ammonia. (*A*) Representative Western blots show no change in intracellular TSP-1 level when astrocytes were treated with 0.5 and 1.0 mM ammonia for 5 days. However, intracellular TSP-1 level declined when astrocytes were exposed to 2.5 mM ammonia for 5 days. (*B*). Quantification of NH_4Cl-induced changes in TSP-1 protein expression. TSP-1 levels were normalized against α-tubulin. (*C*) TSP-1 mRNA levels were decreased after ammonia treatment. *$p<0.05$ vs. control. C, control; N, NH_4Cl.

FIGURE 3. TGF-β1 level after a 10-day treatment of cultured astrocytes with 1.0 mM ammonia. (*A*) Representative Western blots from ammonia-treated astrocytes show a significant decrease in intracellular TGF-β1 level. (*B*) Quantification of NH_4Cl-induced changes in TGF-β1 protein level (n=4). *$p<0.05$ vs. control. C, control.

FIGURE 4. Immunocytochemistry of synaptophysin in cultured neurons. (*A-D*). Astrocytes were treated with ammonia (0.5-2.5 mM) for 10 days and the conditioned media (CM) was then added to neurons for 24 h. Such treatment caused a significant loss in neuronal synaptophysin levels in a dose-dependent manner. (*E*). Quantification of synaptophysin level in neurons after exposure of cells to CM from ammonia-treated astrocytes. *$p<0.05$ vs. control. Scale bar = 30 μm. C, control.

FIGURE 5. Effect of antioxidants and the NF-κB inhibitor (SN50) on extracellular TSP-1 levels in cultured astrocytes. Astrocytes were pretreated (15 min) with antioxidants dimethylthiourea (DMTU; 100 μM, a potent scavenger of hydroxyl radicals), Mn(III) tetrakis (4-benzoic acid) porphyrin (MnTBAP; 10 μM, a selective scavenger of superoxide), L-NAME (250 μM, inhibitor of NOS) and SN50 (0.5-1.0 μM, inhibitor of NF-κB) and then exposed to ammonia (1.0 mM) for 24 h, and TSP-1 levels were measured. Representative Western blots showed that antioxidants (MnTBAP and DMTU and L-NAME (*A*), as well as SN50 (*B*), significantly reduced the inhibition of TSP-1 level after ammonia treatment. The antioxidant MnTBAP, and the NOS inhibitor L-NAME also significantly reduced the inhibition of TSP-1 mRNA by ammonia (*C*). *$p<0.05$ versus control; †$p<0.05$ versus NH_4Cl. C, control; A, ammonia (NH_4Cl); M, MnTBAP; LN, L-NAME; D, DMTU.

Suppl Fig. 1

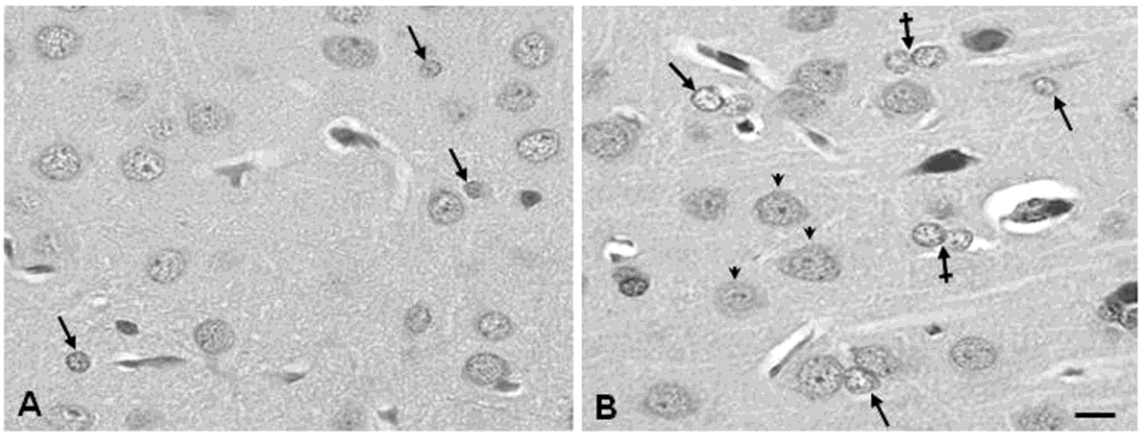

Suppl Fig. 2

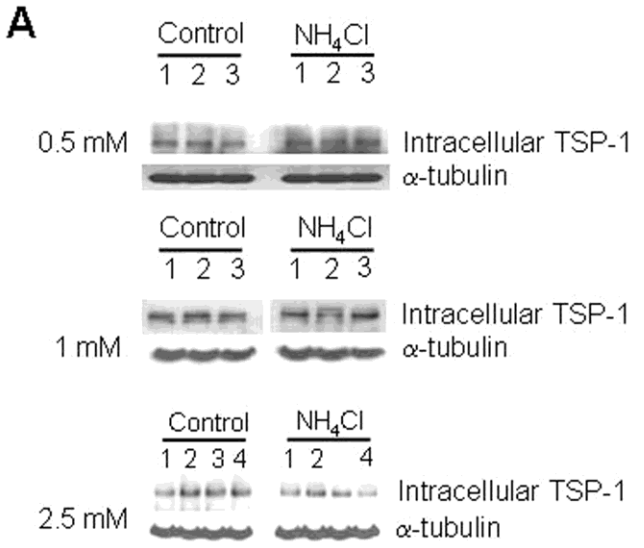
A
Control
NH4Cl
1 2 3
1 2 3
0.5 mM
Intracellular TSP-1
α-tubulin
Control
NH4Cl
1 2 3
1 2 3
1 mM
Intracellular TSP-1
α-tubulin
Control
NH4Cl
1 2 3 4
1 2 4
2.5 mM
Intracellular TSP-1
α-tubulin

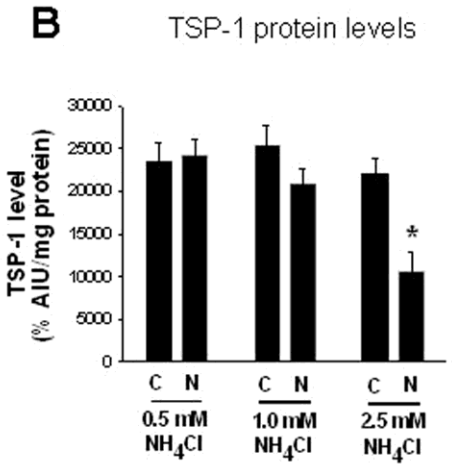
B
TSP-1 protein levels
TSP-1 level
(% AIU/mg protein)
30000
25000
20000
15000
10000
5000
0
C N
0.5 mM
NH4Cl
C N
1.0 mM
NH4Cl
C N
2.5 mM
NH4Cl
*

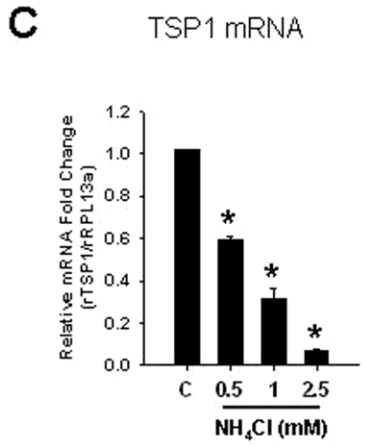
C
TSP1 mRNA
Relative mRNA Fold Change
(rTSP1/rRPL13a)
1.2
1.0
0.8
0.6
0.4
0.2
0.0
C 0.5 1 2.5
NH4Cl (mM)
*
*
*

Suppl Fig. 3

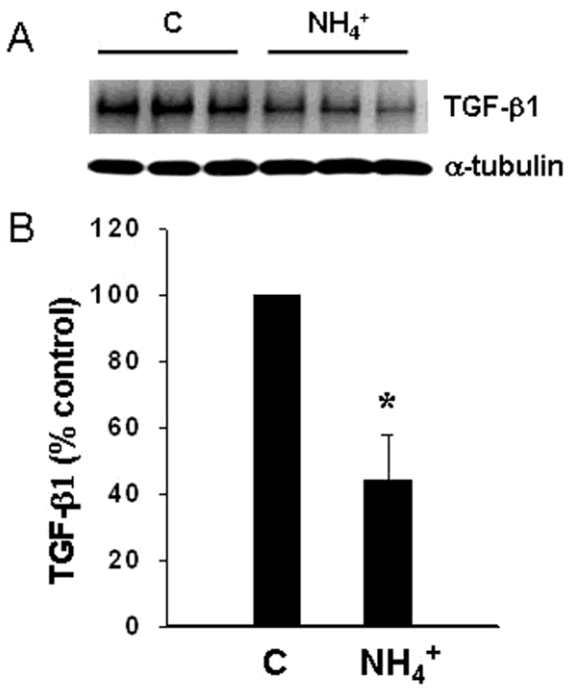
A
C
NH4+
TGF-β1
α-tubulin
B
TGF-β1 (% control)
120
100
80
60
40
20
0
*
C
NH4+

Suppl Fig. 4

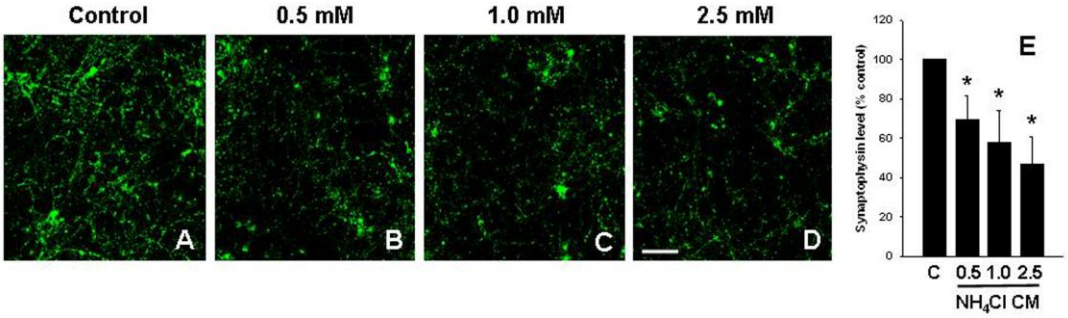
Control
0.5 mM
1.0 mM
2.5 mM
A
B
C
D
E
Synaptophysin level (% control)
120
100
80
60
40
20
0
C
0.5 1.0 2.5
NH4Cl CM

Suppl Fig. 5

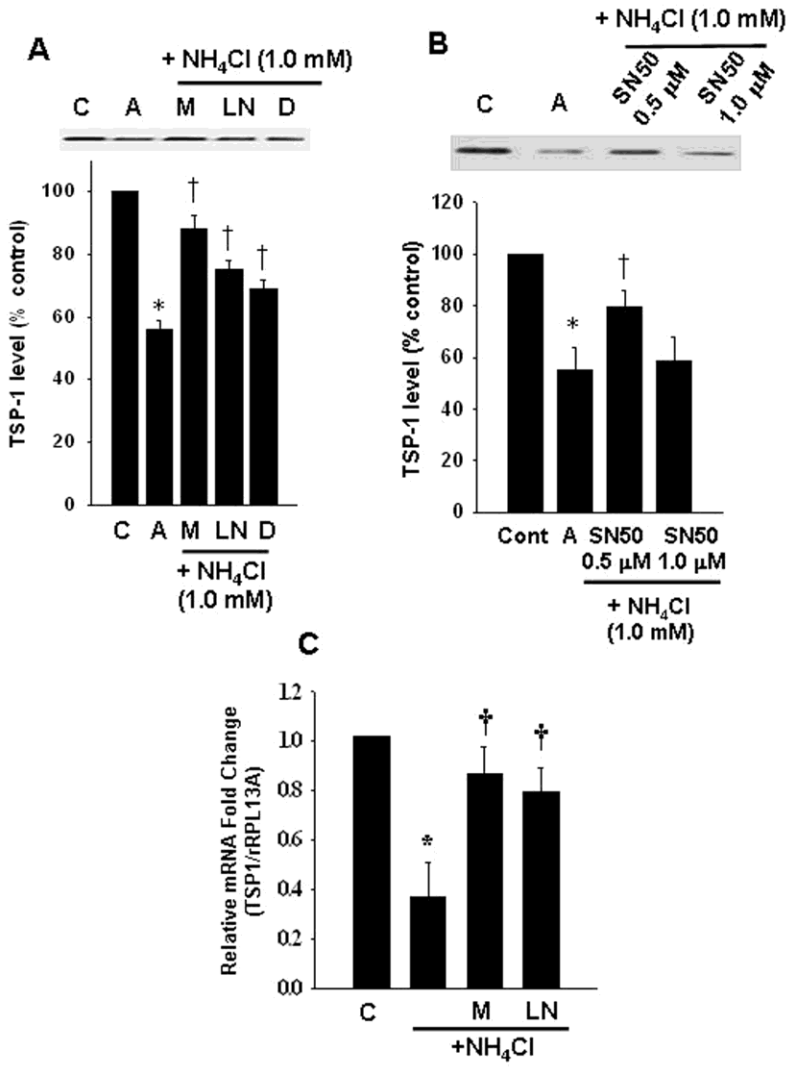
A
+ NH4Cl (1.0 mM)
C A M LN D
TSP-1 level (% control)
100
80
60
40
20
0
C A M LN D
+ NH4Cl
(1.0 mM)
B
+ NH4Cl (1.0 mM)
SN50 0.5 μM
SN50 1.0 μM
C A
120
100
80
60
40
20
0
TSP-1 level (% control)
Cont A SN50 0.5 μM SN50 1.0 μM
+ NH4Cl
(1.0 mM)
C
Relative mRNA Fold Change
(TSP1/rRPL13A)
1.2
1.0
0.8
0.6
0.4
0.2
0.0
C M LN
+NH4Cl